# Self-Diffusion of Polystyrene in a $CO_2$-Swollen Polystyrene Matrix: A Real Time Study Using Neutron Reflectivity

**Ravi R. Gupta,[†] Kristopher A. Lavery,[‡] Timothy J. Francis,[†] John R. P. Webster,[§] Gregory S. Smith,[⊥,#] Thomas P. Russell,[‡] and James J. Watkins*[,†]**

*Department of Chemical Engineering and Department of Polymer Science and Engineering, University of Massachusetts, Amherst, Massachusetts 01003; ISIS, Rutherford Appleton Laboratory, Chilton, Didicot, Oxon, OX11 0QX, U.K.; and LANSCE, Los Alamos National Laboratory, Los Alamos, New Mexico 87545*

*Received July 29, 2002*

ABSTRACT: The self-diffusivities of high molecular weight polystyrene chains in $CO_2$-swollen polystyrene matrices were measured in real time using neutron reflectivity. Bilayer films of hydrogenated and deuterated polystyrene (PS) were prepared on silicon substrates and exposed to compressed $CO_2$. The broadening of the interface between the films as a function of time was determined from the reflectivity profiles, yielding the chain diffusivity. Diffusivity was studied as a function of polymer molecular weight, concentration of $CO_2$ in the polymer film, and temperature. Nearly an order of magnitude enhancement in the diffusivity of polystyrene chains ($M = 2 \times 10^5$), from $1.62 \times 10^{-16}$ to $9.35 \times 10^{-16}$ cm$^2$/s, was found with a modest increase in the concentration of $CO_2$ in the polystyrene (from 8.9 to 11.3 wt %) at 62 °C. This concentration dependence was modeled using the Vrentas−Duda free volume theory. [50−52] At a constant temperature and $CO_2$ pressure the polystyrene diffusivity scaled as $M^{-2.38}$. The scaling of the self-diffusivity of PS in $CO_2$-swollen PS with $T - T_g$, where $T_g$ is the glass transition temperature depressed by the presence of the solvent, is discussed.

## Introduction

Supercritical fluids (SCF's) such as $CO_2$ are effective plasticizing agents for most polymers and upon sorption provide a "solventless" route for polymer modification and processing.[1−4] Although the thermodynamics of block copolymer (BCP) ordering in SCF's has prompted extensive research recently,[5,6] there have been few attempts to understand the dynamics of polymer chains in the presence of $CO_2$. Recently, RamachandraRao et al. showed that $CO_2$ enhances the ordering kinetics in high molecular weight BCP's such as P(S-*b*-MMA), producing structures that are difficult or impossible to achieve by thermal annealing.[7] In the melt, ordering is impeded by slow kinetics due to the high degree of entanglement and the microphase separation of the copolymer. Chain mobility is also an important consideration in the reactive blending of two or more immiscible polymers. In reactive blending, end-functionalized polymer chains diffuse through the respective bulk phases to the interface and react, forming a block copolymer that imparts long-term stability to the blend. The slow dynamics of chains in a high molecular weight polymer matrix causes the reaction to be diffusion-controlled.[8−10] $CO_2$ can be used to increase the mobility of the chains, thereby enhancing the kinetics.[11,12] Recently, Roberts et al. studied the reaction kinetics of the solid-state polymerization of poly(bisphenol A carbonate) swollen with $CO_2$[13] and ascribed the observed enhancement in polymerization rate to increased end-group mobility in the plasticized polymer.

The diffusion of polymers, both in the melt[14−17] and in solution,[18−24] has been widely studied. In the high molecular weight regime ($M > M_e$, where $M_e$ is the entanglement molecular weight) the reptation model, proposed by de Gennes[25] and later modified by Doi and Edwards,[26] captures the basic physics of polymer dynamics. The theory predicts that the viscosity and diffusion coefficient of polymer chains scale with $M^3$ and $M^{-2}$, respectively, for times longer than the characteristic time for a polymer chain to diffuse a distance equivalent to its contour length (the reptation time). This model predicts five distinct time regimes for the mean-square displacement of the chain segment ($g(t)$). For times shorter than the reptation time $g(t) \sim t^{0.25}$. In this regime the entanglements start to influence the dynamics of chain segments relaxing via Rouse modes. At times longer than reptation time, the random walk result is recovered with $g(t) \sim t$. Over the past two decades, numerous studies have been performed to test this model.[27−29] Using IR microdensitometry, Klein showed that for high molecular weights polyethylene diffusivity scaled as the inverse square of the molecular weight.[30] Richter et al., using spin echo spectroscopy and rheometry, showed the existence of an intermediate length scale in melts of poly(ethylene−propylene) that reduced the relaxation of the density fluctuation of the chains.[31] Also, the intermediate length scale was in excellent agreement with the entanglement distance predicted from reptation theory. Russell et al. used dynamic secondary-ion mass spectrometry (DSIMS) to demonstrate that polystyrene chains diffuse across the interface in a curvilinear motion, which supports the tenets of reptation.[32] Using Rutherford backscattering and forward recoil spectrometry, Green et al. studied

[†] Department of Chemical Engineering, University of Massachusetts.
[‡] Department of Polymer Science and Engineering, University of Massachusetts.
[§] Rutherford Appleton Laboratory.
[⊥] Los Alamos National Laboratory.
[#] Presently at HFIR Center for Neutron Scattering, Oak Ridge National Laboratory, Oak Ridge, TN 37831.
* To whom correspondence should be sent: e-mail watkins@ecs.umass.edu.

10.1021/ma021215r CCC: $25.00 
Published on Web 12/28/2002

**Table 1. Weight-Average Molecular Weights ($M_w$) and Polydispersities of DPS and HPS Samples Used in This Study**

| polymer | $M_w$ (g/mol) | $M_w/M_n$ | polymer | $M_w$ (g/mol) | $M_w/M_n$ |
|---|---|---|---|---|---|
| HPS-100K | 102 000 | 1.04 | HPS-300K | 293 000 | 1.04 |
| DPS-100K | 110 500 | 1.03 | DPS-300K | 333 900 | 1.05 |
| HPS-200K | 228 000 | 1.05 | HPS-600K | 629 800 | 1.12 |
| DPS-200K | 217 600 | 1.04 | DPS-600K | 577 000 | 1.04 |

self-diffusivity and tracer diffusivity of polystyrene at 174 and 171 °C, respectively. The molecular weight of the polystyrene chains ranged from 33 000 to 943 000 g/mol. Their results indicate polystyrene diffusivity scales as $M^{-2}$ in keeping with reptation arguments.[16,33] These authors also found[17] that the temperature dependence of the tracer diffusion coefficient of high molecular weight PS could be described by the Vogel equation.[34]

There is extensive literature describing polymer diffusion in polymer−liquid solvent systems. Using forced Rayleigh scattering (FRS), Leger et al. showed that the self-diffusion coefficient ($D_S$) of polystyrene in a good solvent, in semidilute solutions, scales as $c^{-1.7}M^{-2}$, in near exact agreement with reptation arguments where $D_S \sim c^{-1.75}M^{-2}$.[21,35,36] Wesson et al., in a study of the self-diffusion of polystyrene in THF in the semidilute to concentrated regimes, also found $D_S \sim M^{-2}$.[22] However, the concentration dependence of $D_S$ agreed with the predictions of the Rouse model. Nemoto et al., in a study of entangled polystyrene solutions of dibutyl phthalate (DBP),[23,24] found that $\eta = M^{3.5\pm0.1}$ and $D_S = M^{-2.5}$ also in agreement with the reptation arguments. More recently, however, the scaling predictions of reptation theory have been questioned. In highly entangled polybutadiene melts and solutions, $D_s \sim M^{-2.3\pm0.1}$, which disagrees with reptation predictions for entangled systems but is consistent with the scaling of viscoelasticity in polymer solutions and melts.[37,38]

Various techniques have been used to measure dynamics in polymer systems. Neutron reflectivity (NR), with a depth resolution of ∼1 nm, offers a number of advantages for measuring a wide variety of interfacial phenomena including diffusion of polymer chains.[39] Recently, Bucknall et al. conducted real time NR measurements of polystyrene diffusion at 115 °C, at ambient pressure.[40] The interfacial width between layers of deuterated polystyrene (DPS) and hydrogenated polystyrene (HPS) bilayer exhibited a time dependence of $t^{1/4}$ at initial stages to $t^{1/2}$ at long annealing times consistent with the reptation.[25,41] The same study showed highly asymmetric interfacial profiles for the diffusion of oligomeric styrene into high MW polystyrene at 65 °C.

Here the chain mobility in PS films dilated with $CO_2$ is described. Real time measurements are required for the accurate measurement of chain diffusivity in $CO_2$-swollen polymer films, since stopped time measurements require the depressurization of the sample after annealing. This can lead to a cavitation of the polymer and to a distortion of the interface between the polymer layers, causing erroneous results.

## Experimental Section

Narrow molecular weight distribution PS samples were purchased from Polymer Source Inc., Dorval, PQ, Canada. The weight-average molecular weights and polydispersities are listed in Table 1. Silicon wafers were purchased from International Wafers Service Inc., Portola Valley, CA, and were cut into 2 in. × 2 in. squares. Deuterated PS (DPS) and hydrogenated PS (HPS) films were spin-coated from toluene solution onto cleaned silicon wafers (with the native oxide) and onto cleaned glass slides, respectively. Film thickness was measured using optical ellipsometery (Rudolph AutoEl 2). DPS films on silicon wafers were subsequently annealed in a vacuum oven at 160 °C for 16−20 h to relax stresses developed during the spin-coating process. A bilayer film was prepared by floating the HPS film onto a pool of deionized water and transferring it on top of the DPS film. The bilayer was dried under vacuum at 65 °C for 4−5 h to remove water from the interface.

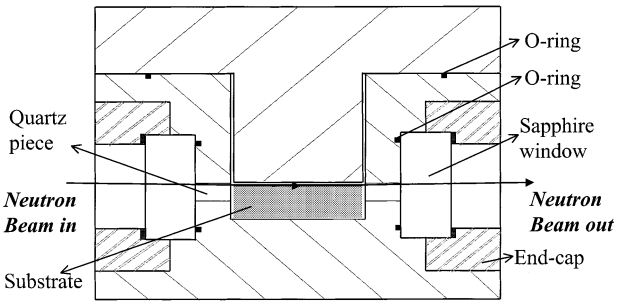


**Figure 1.** Schematic of the high-pressure neutron reflectivity cell.

Neutron reflectivity experiments were performed using a custom-built high-pressure cell (Figure 1) consisting of two stainless steel flanges bolted together and sealed with a Teflon O-ring. The cell accommodates the bilayer samples on 2 in. × 2 in. silicon wafers. The neutron beam is transmitted through a series of sapphire windows (1.6 in. diameter and 0.6 in. thick) and small quartz spacers. The spacers are used to reduce the scattering of the neutron beam by the compressed fluid. The cell is heated with cartridge heaters and is insulated by a Garolite box. High-pressure $CO_2$ is supplied through a computer-controlled syringe pump (ISCO Products Inc.). The pressure of the system within the sample chamber is measured directly. The sapphire windows are secured to the main cell body by two threaded stainless steel end-caps and sealed with Teflon O-rings. Experiments were performed from 62 to 85 °C at $CO_2$ fluid pressures up to 125 bar. Both the SURF reflectometer at ISIS, Rutherford Appleton Laboratory, UK, and the SPEAR reflectometer at LANSCE, Los Alamos National Laboratory, NM, were used in this study. NR data were collected on SURF from $k = 0.0075$ to 0.0235 Å$^{-1}$, whereas the data collected at SPEAR covered a $k$ range from 0.005 to 0.0325 Å$^{-1}$ ($k = (2\pi/\lambda)\sin(\theta)$ where $\lambda$ is the wavelength and $\theta$ is the grazing angle of incidence). On both instruments the data acquisition time ranged from 3 to 5 min per reflectivity curve. Because of the presence of high-pressure windows and $CO_2$, there was a wavelength-dependent attenuation of the neutrons that was taken into account by the measurement of the neutron spectrum with and without a $CO_2$-filled cell. The reflectivity curves were fit to a bilayer model using an error function to define the root-mean-square (rms) roughness between the HPS and DPS layers. The error function representation of the interfacial roughness is justified because in all the experiments the total thickness of the bilayer films was ∼2000 Å, which is more than an order of magnitude larger than the maximum rms roughness observed between the polymer layers (∼130 Å). Interfacial width was then calculated on the basis of the rms roughness (see Results and Discussion).[42,43] By design, fitting the reflectivity profiles required fitting only three parameters: the rms roughness between the polymer layers and $\Delta k/k$, which contains resolution in $\lambda$ ($\Delta\lambda/\lambda$) and $\theta$ ($\Delta\theta/\theta$).

## Results and Discussion

A typical set of in situ, real time reflectivity profiles is shown in Figure 2. The example is data from a bilayer film of PS (200K) at 62 °C and 83 bar of $CO_2$ pressure.

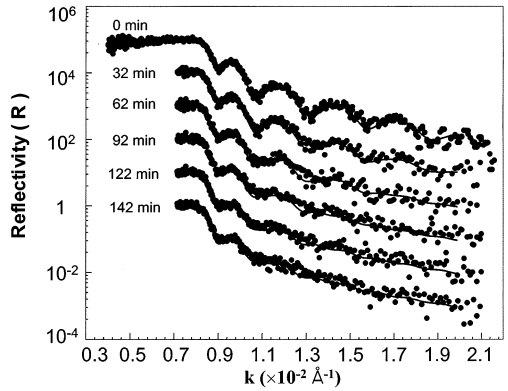


**Figure 2.** Set of reflectivity profiles for the bilayer film, HPS/DPS (200K). The profiles were obtained at 62 °C and 83 bar. Each reflectivity profile was acquired for 5 min. The time shown on the left is the elapsed time prior to collection of each reflectivity profile. The solid line is the bilayer model.

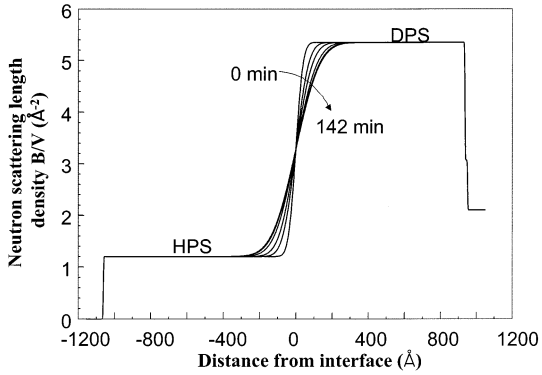


**Figure 3.** Neutron scattering length density variation with time. The sample and conditions are the same as in Figure 2. The arrow indicates increasing time from 0 to 142 min.

Upon sorption of $CO_2$, the critical edge of the PS film shifts from $k = 0.0089$ Å$^{-1}$ at 62 °C and ambient pressure to $k = 0.0082$ Å$^{-1}$ at 62 °C and 83 bar. The film thickness increases by ~12% upon $CO_2$ sorption. Reflectivity profiles were also obtained, in real time, for a 100 nm thick DPS film on silicon substrate upon sorption of $CO_2$ under similar conditions. Profiles, acquired every 4 min, showed no changes over a period of 2 h, indicating that the PS−$CO_2$ system reached equilibrium very rapidly. It is assumed that there were no specific interactions between $CO_2$ and PS chains. Consequently, the diffusivities measured are essentially the self-diffusivities of the chain.

The data in Figure 2 show that the amplitudes of the fringes decay with time as a result of interfacial broadening. The evolution of the concentration profiles used to fit these data is shown in Figure 3. For times in excess of the reptation time, the interfacial width should increase linearly with time. Figure 4 shows the time dependence of the square of the interfacial width, which satisfies this prediction. Interfacial widths ($a_i$) are computed from the rms roughness ($\sigma$), between the layers, via $a_i = \sqrt{2\pi\sigma}$. The rms roughness at a time $t$ was corrected quadratically for the initial rms roughness that arose from the sample preparation technique.[43] Since experiments were performed at times greater than the reptation time, distinguishing between reptation or any other mode of diffusion was not possible.

The self-diffusivity of the PS chain can be directly computed from the slope of the line in Figure 4. The

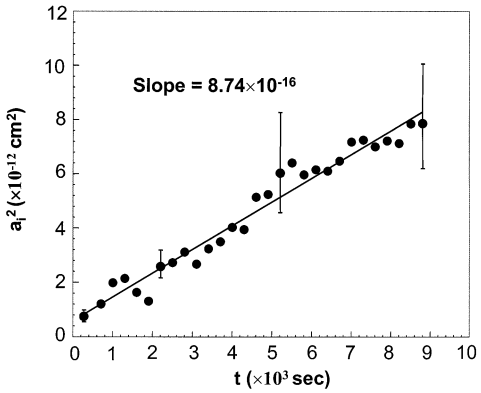


**Figure 4.** Square of interfacial width vs annealing time. The slope is directly proportional to the self-diffusivity of the PS chains. The sample and conditions are the same as in Figure 2. The error bars are based on 5% deviation from the best-fit value for the given reflectivity profile. Zero time is the onset of data collection, which is slightly time-shifted from the onset of interfacial broadening (see text).

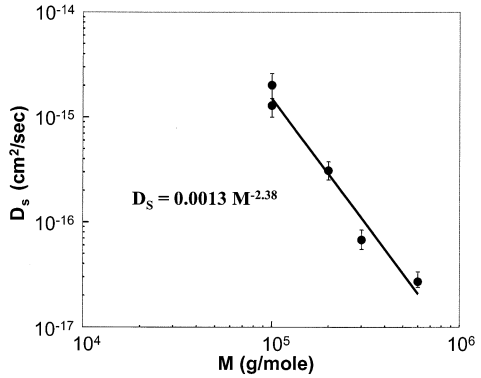


**Figure 5.** Self-diffusivity of PS as a function of molecular weight. The temperature and fluid phase pressure are 62 °C and 90 bar, respectively.

square of the interfacial width is related to the annealing time (at long times) via

$$a_i^2 = 4D_S t \qquad (1)$$

where $a_i$ is the interfacial width between the polymer layers, $t$ is the time, and $D_S$ is the self-diffusivity of PS chains, which is dependent solely on the slope of the line in Figure 4. Data acquisition was started after the pressure at a particular temperature stabilized to a final value. We denote the onset of the data acquisition as $t = 0$. During the period of equilibration, prior to $t = 0$, the interface broadened to a finite width. Therefore, eq 1 is not forced through the origin in Figure 4 as at time zero there is a finite interfacial width between the polymer layers. The self-diffusivity of PS chains (200K) for the conditions described above was found to be 2.19 × 10$^{-16}$ cm$^2$/s using the slope of the data in Figure 4.

**A. Molecular Weight Dependence.** Four different PS molecular weights (Table 1), covering approximately half a decade, were used to obtain the molecular weight dependence of self-diffusivity. Experiments were conducted at $T = 62$ °C and $P_{CO_2} = 90$ bar, hence at constant $CO_2$ concentration in PS. A plot of $D_S$ as a function of molecular weight is shown in Figure 5, yielding an exponent of −2.38. This is in agreement with data for PS diffusivities in concentrated solutions of organic solvents[23,24] and shows a stronger dependence on molecular weight than that seen in the melt or

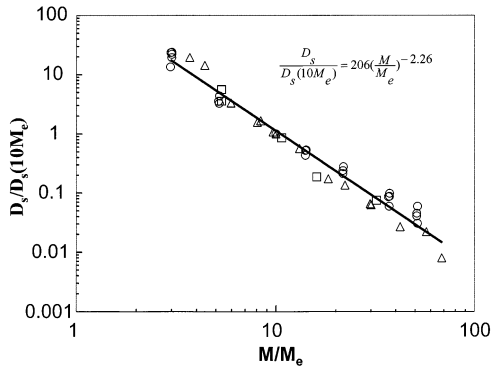


**Figure 6.** Diffusivity vs molecular weight. The diffusivity is scaled with its value at $10M_e$: data from this study at 62 °C and 90 bar (□), data from Nemoto et al. for PS in DBP (△),[23,24] and data from Green et al. for PS melt (○).[16] The solid line is the best-fit line through all the data.

predicted by the reptation model. It is well established that the viscosity and the associated relaxation time, for molten polymers and concentrated polymer solutions, vary as $M^{3.4}$.[24,44] If the diffusivity and the viscosity are "intimately related" and, therefore, characterized by the same relaxation time,[37] then the self-diffusivity at times longer than the characteristic relaxation time should vary as $M^{-2.4}$. The disagreement of the exponent with the reptation theory, where an exponent of −2 is predicted, can be resolved if restrictions of the theory are relaxed.[24,27,37,38]

The ratio of $D_S(M,T,C)$ to $D_S(10M_e,T,C)$ was plotted as a function of $M/M_e$ in Figure 6.[37,38] Here, $D_S(10M_e,T,C)$ is the self-diffusivity of PS chains at the same temperature and solvent concentration but at a molecular weight 10 times that of the entanglement value. Following the recipe of Lodge et al.,[37,38] reducing the variables in this manner elucidates the dependence of self-diffusivity on molecular weight explicitly, as there is no contribution from the friction factor (assuming its dependence on $M$ is small at $M \gg M_e$ (see section C)). To check for universality in the molecular weight exponent ($M > M_e$) of polymer self-diffusivity, in melts and solutions, Figure 6 compares data from this study with the data for molten PS[16] and in concentrated solutions of PS in dibutyl phthalate (DBP).[24] The value of $D_s(10M_e,T,C)$ at $10M_e$ for each data set was obtained by interpolating the data. A best-fit line through the composite data set yields an exponent of −2.26, very close to the published value of −2.28.[37,38] Using only the data obtained in this study, an exponent of −2.38 was found.

It is important to note that the entanglement molecular weight for the PS−$CO_2$ system was calculated using the empirical equation for concentrated PS solutions[45]

$$M_e = 1.8 \times 10^4 c^{-1} \tag{2}$$

where $c$ is the polymer concentration in g/cm$^3$. The polymer concentration in our case was calculated using the Sanchez−Lacombe equation of state (S−L EOS) with interaction parameters obtained by fitting the experimentally determined sorption isotherms. In this study we use $CO_2$ sorption data in PS recently measured at 65 °C and pressures between 61 and 102 bar, above the glass transition pressure of the system, using high-pressure neutron reflectivity.[46]

**Table 2. Vrentas−Duda Free Volume Parameters**

A. Critical Hole Free Volume at 0 K and Hole Free Volume at 62 °C

| | $CO_2$ | PS monomer repeat unit |
|---|---|---|
| $\hat{V}_i^*$, cm$^3$/g | 0.589 | 0.85 |
| $V_i^H$, cm$^3$/g | 0.25 | 0.024 |

B. Fit Parameters

| | this study | literature |
|---|---|---|
| $\xi$ | 0.233 | 0.187 |
| $D_{0_s}$ | $1 \times 10^{-6}$ | |

**B. Concentration Dependence.** Free volume is an important parameter in determining the rate of molecular motion in polymer systems.[44] The concept of free volume is based on Cohen−Turnbull theory, which relates the molecular mobility in hard sphere liquids to the free volume of the system.[47,48] Here, a molecule jumps into a void created due to nonenergetic redistribution of the free volume when such a void reaches a critical size. Fujita applied this concept to predict mobility in polymer−diluent systems.[49] Subsequently, Vrentas and Duda derived a more robust free-volume-based model that describes the diffusivity of diluents and polymer chains in polymer mixtures over a wide range of concentrations and temperatures.[50−52] According to this model, the diffusivity of polymer chains in a binary mixture with a solvent is given by[52]

$$D_S = D_{0S} \exp\left(-\frac{\gamma(w_1\hat{V}_1^* + w_2\hat{V}_2^*\xi)}{\hat{V}_{FH}\xi}\right) \tag{3}$$

where $D_S$ is the self-diffusivity of polymer; $D_{0S}$ is the preexponential factor, which incorporates the effect of temperature; $w_i$ and $\hat{V}_i^*$ are the weight fraction and the critical hole free volume per gram for the displacement of the $i$th jumping segment. $\hat{V}_{FH}$ is the average hole free volume per gram of the mixture. If the volume change on mixing is assumed to be small, $\hat{V}_{FH}$ can be obtained by adding the free volume of the respective components of the mixture weighted over the weight fractions of the individual components. $\gamma$ is the overlap factor signifying that more than one jumping unit can occupy a site. $\xi$ is the ratio of the jumping units of the solvent and polymer segments and is given by

$$\xi = \frac{\hat{V}_1^0(0)M_1}{\hat{V}_2^0(0)M_j} \tag{4}$$

where $M_1$ and $M_j$ are the molecular weights of the jumping units of the solvent and polymer, and $\hat{V}_i^0(0)$ is the specific occupied volume of the $i$th component at 0 K. All parameters except $D_{0S}$ and $\xi$ were obtained from the literature. The methodology for calculating the parameters is shown in the Appendix, and the results are given in Table 2A. The Vrentas−Duda free volume theory describes the self-diffusivity of the PS chains in $CO_2$-swollen polystyrene remarkably well over the concentration range studied (Figure 7). The two parameters $D_{0S}$ and $\xi$ were used to fit the self-diffusivity−concentration data to the model. The data in Figure 7 were obtained for PS(200K) at 62 °C and $CO_2$ pressure range of 76−104 bar. The fitting parameters are listed in Table 2B. The value of $\xi = 0.233$ is in reasonable agreement with others.[53] If it is assumed that the $CO_2$ diffuses as a whole molecule, the jumping unit for the

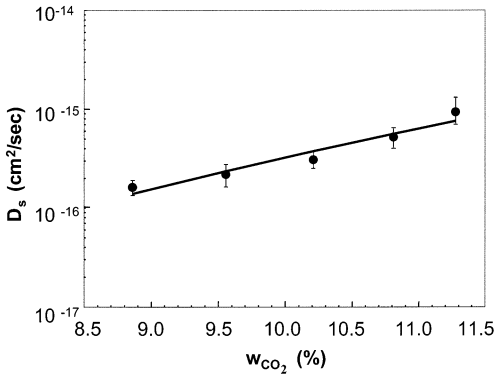


**Figure 7.** Variation of PS self-diffusivity with $CO_2$ concentration in the PS matrix. The solid line is from the Vrentas−Duda free volume model. Concentration in weight percent ranges from 8.9% to 11.3%.

PS segment calculated using eq 4 is 1.25 times the monomer molecular weight (104 g/mol). The specific occupied volumes for $CO_2$ and the PS jumping segment at 0 K were assumed to be equal to their van der Waals volume at 0 K (see Appendix). The parameters used in this study were found to yield accurate description of the probe diffusion in $CO_2$-dilated matrices using the Vrentas−Duda equation.[54]

As shown in Figure 7, diffusivity increases by nearly an order of magnitude, from $1.62 \times 10^{-16}$ to $9.35 \times 10^{-16}$ $cm^2/s$, upon modest increase in the concentration of $CO_2$ in the polystyrene matrix from 8.9 to 11.3 wt % at 62 °C. At 62 °C and a solvent loading of 8.9%, the PS−$CO_2$ system is ∼28 °C above the glass transition temperature. Using the parameters obtained in this study, the Vrentas−Duda model (eq 3) can be used to predict the diffusivity of PS over a range of solvent loadings. For example, at $T = 62$ °C and $P_{CO_2} = 40$ bar, PS diffusivity is predicted to be $2.3 \times 10^{-18}$ $cm^2/s$. At these conditions, the PS−$CO_2$ system is ∼5 °C above the ambient pressure glass transition temperature (see section C).

**C. Temperature Dependence.** The diffusivity of a polymer chain can be described by[29]

$$D_s = g(c,M)f^{-1}(\zeta(c,M,T)) \tag{5}$$

The function $g$ incorporates topological effects and is dependent on $M$ and $C$. It characterizes the effect of entanglement on the chain mobility. The temperature dependence of diffusivity is embedded in the friction coefficient, $f$. The effect of molecular weight on the friction coefficient is negligible for high molecular weight polymers,[44] but $f$ is strongly dependent on the concentration. To elucidate the effect of temperature on the friction coefficient, it is useful to plot the reduced diffusivity, $D_S M^{\alpha}/T$ vs $T$ or $T - T_g$, where α is the exponent for the molecular weight dependence of the diffusivity (see section A).[17] It is well-known that sorption of $CO_2$ in polymers leads to depressions in the glass transition temperature.[55] At a given temperature ($T$) and $CO_2$ pressure the system will possess a unique glass transition temperature ($T_g$). Therefore, the polymer−$CO_2$ system at a particular $T$ and $c$ can be mapped onto an equivalent $T - T_g$ scale.[56] This implies that the polymer solution can be treated as a melt at a temperature of $T - T_g$ above the glass transition temperature of the pure polymer. The scaled self-diffusivity was plotted with respect to $T - T_g$ in Figure 8. $CO_2$ concentrations at a particular temperature and fluid pressure were calculated as described in section A. The glass transition temperature was calculated from Chow's model[57]

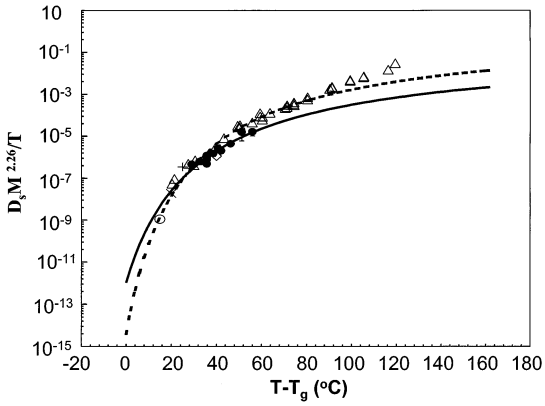


**Figure 8.** Scaled diffusivity vs $T - T_g$: data from this study (●), data from Green et al. (△),[33] data from Bucknall et al. (○),[40] data from Karim et al. (×),[43] data from Whitlow et al. (+),[61] data from Steiner et al. (◇).[60] The solid and the dashed lines are the best fits of the Vogel equation to our data set and to all the data, respectively.

$$\ln\left[\frac{T_g}{T_g(w_d=0)}\right] = \beta[(1-\theta)\ln(1-\theta) + \theta\ln(\theta)] \tag{6}$$

$$\theta = \alpha\left[\frac{w_d}{1-w_d}\right] \tag{7}$$

where $w_d$ is the weight fraction of the $CO_2$ in the polystyrene matrix; $\beta$ and α are system-dependent constants. The values of the latter parameters ($\beta$ = 0.635 and α = 0.972) were obtained from the literature.[58,59] Results obtained in this study were compared with data for PS diffusivity in the melt phase obtained using other techniques.[17,40,43,60,61] The molecular weight exponent used in all the cases was 2.26, as shown in section A. Most of the data obtained in this study are slightly lower than the data in the melt phase, suggesting that the friction coefficient is slightly higher in PS−$CO_2$ than in the melt. This is counterintuitive and may suggest that the concentration dependence of the friction coefficient does not scale with $T - T_g$ alone. However, it is important to note that there is some uncertainty in the calculation of the depression in $T_g$ due to $CO_2$ sorption.

The data in Figure 8 can also be correlated using free-volume-based model relating $D_s$ to $T - T_g$. The free-volume-based Vogel equation describes the viscoelastic properties of polymer melts and solutions and is given by[34]

$$\ln\left(\frac{D_s M^{\alpha}}{T}\right) = A - \frac{B}{T - T_{\infty}} \tag{8}$$

where $A$, $B$, and $T_\infty$ are empirical parameters that are usually obtained by fitting the experimental data. $B$ was fixed at a value of 780.[34] In Figure 8 the dashed curve is the Vogel equation fit to all the experimental data over a $T - T_g$ range of 15−100 °C. Deviations above 80 °C between the fit and the data are not surprising due to the inability of the free-volume-based models to describe dynamics at temperatures far removed from the glass transition temperature.[44] The values of the

**Table 3. Comparison of the Empirical Constants in Vogel Equation from This Study with Published Results**

| | *B* | *A* | $T_\infty$ (°C) |
|---|---|---|---|
| all data | 780 | 0.902 | 76.4 |
| our data | 780 | 0.123 | 69.4 |
| Green et al.[33] | 710 | | 49 |
| Fox and Berry[34] | 780 | | 40 |

fitting parameters are compared with the literature values in Table 3. The solid line in Figure 8, with slightly different set of parameters (Table 3), is fit to the data obtained in this study.

Assuming Arrhenius behavior, an apparent activation energy ($E_{ac}$) of 140 kJ/mol was evaluated for PS self-diffusivity (600K) in $CO_2$-swollen PS matrix at a constant volume fraction of 0.074 from 62 to 85 °C. In the melt Green et al., determined activation energies of 226 and 254 kJ/mol for molecular weights of 55 000 and 110 000 g/mol, respectively (Figure 9).[17] Since the apparent activation energy is usually a function of temperature, it is meaningful to compare the values over a similar $T - T_g$ range. The $T - T_g$ in Figure 9 ranges from 30 to 60 °C. The disparity of 85−110 kJ/mol in the apparent activation energy for PS chains in PS−$CO_2$ compared to the PS melt can be rationalized in terms of the lower segmental friction and higher probability for critical void formation in the presence of the $CO_2$. The above arguments point to the inability of $T - T_g$ scaling to completely account for the concentration dependence of the friction factor.

## Conclusion

The self-diffusivity of PS chains in a $CO_2$-swollen PS matrix was studied as a function of temperature, $CO_2$ concentration, and molecular weight. Real time experiments were performed in situ, using high-pressure NR. The study indicates a scaling of the self-diffusivity $D_s \sim M^{-2.38}$, which is in good agreement with that obtained in organic solvents. The molecular weight scaling of self-diffusivity in systems ranging from polymer−organic solvents to polymer−$CO_2$ provides confidence in the universality of the exponent. The measurements demonstrate nearly an order of magnitude increase in the diffusivity upon increase of the sorbed volume fraction of $CO_2$ from 8.9 to 11.3 wt % at 62 °C. The self-diffusivity of PS at 62 °C and 40 bar predicted using Vrentas−Duda free volume model indicates that $CO_2$ is an effective plasticizing fluid. The diffusivity increases by about 2 orders of magnitude upon sorption of $CO_2$ at 62 °C and 77 bar in comparison to 62 °C and 40 bar, conditions at which the PS−$CO_2$ system is ~5 °C above the glass transition temperature of PS at ambient pressure. The range of diffusivities studied varied by nearly 2 orders of magnitude from $2.7 \times 10^{-17}$ to $2 \times 10^{-15}$ cm$^2$/s. To extend the study to measure higher diffusivities in PS−$CO_2$ systems, other techniques such as fluorescence nonradiative energy transfer or forced Rayleigh scattering technique will be required.

**Acknowledgment.** The authors acknowledge the NSF Materials Research Science and Engineering Center at University of Massachusetts Amherst for providing the financial support. The authors are greatly indebted to Dr. Stephen Holt, the staff at the SURF reflectometer, ISIS, and the staff at the SPEAR reflectometer, LANSCE, for providing support and helpful suggestions during the course of the experiments. The authors also acknowledge Dr. A. Taylor, Director of ISIS, for providing discretionary time to establish the feasibility of these measurements.

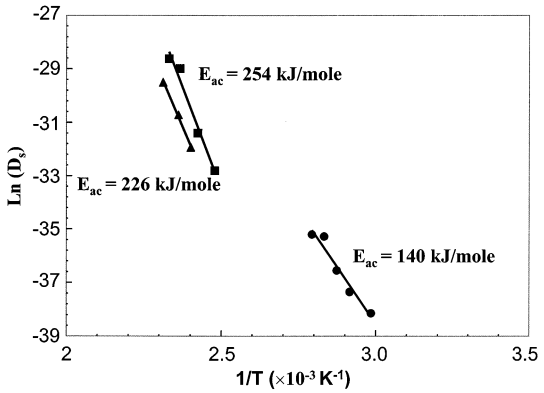


**Figure 9.** Plot of ln($D_s$) vs the inverse of absolute temperature: this study at a constant volume fraction of 0.074 of $CO_2$ in PS (600K) (●), data from Green et al. for PS ($M$ = 50 000 g/mol) (■), data from Green et al. for PS ($M$ = 110 000 g/mol) (▲).[17] The solid line assumes Arrhenius behavior.

## Appendix

The following assumptions are made in order to calculate the free volume parameters for $CO_2$ and the monomer repeat unit of PS: (a) The hole free volume and the interstitial volume vary linearly with temperature. (b) The hole free volume for the mixture can be obtained by adding the hole free volumes of the pure component weighted over the respective weight fractions in the mixture. (c) The hole free volume thermal expansion coefficient is independent of temperature. (d) The critical hole free volume $\hat{V}_i^*$ is equal to the van der Waals volume at 0 K.

A detailed recipe for free volume parameter evaluation can be obtained from other sources.[62] In the case of $CO_2$ the critical hole free volume $\hat{V}^*_{CO_2} = 0.589$ cm$^3$/g was obtained from the literature.[53] The hole free volume thermal expansion coefficient for $CO_2$ is calculated from the known solid and liquid densities at the triple point of $CO_2$ and the van der Waals volume of $CO_2$ at 0 K.[62] The value comes out to be $8.76 \times 10^{-4}$ cm$^3$/(g K). The value of the hole free volume for $CO_2$ at 62 °C is calculated using the equation

$$V^H_{CO_2}(T) = V^H_{CO_2}(40\ °C) + 8.76 \times 10^{-4}(T - 40) \quad (9)$$

where the $V^H_{CO_2}(40\ °C) = 0.231$ cm$^3$/g is obtained from Alsoy et al.[53] The value for $V^H_{CO_2}(62\ °C)$ comes out to be 0.25 cm$^3$/g. The overlap factor $\gamma$ is assumed to be equal to 1.0.

Similarly, in the case of PS monomer repeat unit the critical hole free volume $\hat{V}^*_{PS,repeatunit} = 0.85$ cm$^3$/g is obtained from the literature.[53] The thermal expansion coefficient for the hole free volume is calculated assuming a universal value of 0.025 for the free volume fraction at the glass transition temperature. The value is calculated to be $6.54 \times 10^{-5}$ cm$^3$/(g K). The hole free volume for the PS repeat unit at 62 °C is calculated using an equation similar to (9), and $V^H_{PS,repeatunit}(40\ °C) = 0.0225$ g/cm$^3$, obtained from Alsoy et al.[53] The overlap factor was assigned a value of 1.0. The value for the hole free volume for the PS repeat unit at 62 °C comes out to be 0.0239 g/cm$^3$.

Finally, the average hole free volume fraction for the mixture per gram is calculated using the following equation:

$$\hat{V}_{FH}(62\ °C) = w_1 V^{H}_{CO_2}(62\ °C) + w_2 V^{H}_{PS,\text{repeat unit}}(62\ °C) \quad (10)$$

## References and Notes


(1) Watkins, J. J.; McCarthy, T. J. *Macromolecules* **1994**, *27*, 4845−4847.
(2) Watkins, J. J.; McCarthy, T. J. *Chem. Mater.* **1995**, *7*, 1991−1994.
(3) Watkins, J. J.; McCarthy, T. J. *Macromolecules* **1995**, *28*, 4067−4074.
(4) Brown, G. D.; Watkins, J. J. *Carbon Dioxide-Dilated Block Copolymer Templates for Nanostructured Materials; MRS Proc.* **2000**, *584*, 169−174.
(5) Vogt, B. D.; Brown, G. D.; RamachandraRao, V. S.; Watkins, J. J. *Macromolecules* **1999**, *32*, 7907−7912.
(6) Watkins, J. J.; Brown, G. B.; RamachandraRao, V. S.; Pollard, M. A.; Russell, T. P. *Macromolecules* **1999**, *32*, 7737−7740.
(7) RamachandraRao, V. S.; Gupta, R. R.; Russell, T. P.; Watkins, J. J. *Macromolecules* **2001**, *34*, 7923−7925.
(8) Fredrickson, G. H. *Phys. Rev. Lett.* **1996**, *76*, 3440−3443.
(9) Fredrickson, G. H.; Miller, S. T. *Macromolecules* **1996**, *29*, 7386−7390.
(10) O'Shaughnessy, B.; Sawhney, U. *Phys. Rev. Lett.* **1996**, *76*, 3444−3447.
(11) Ortelli, D. E. Reactive Polymer Blending in Supercritical Carbon Dioxide. M.S. in Chemical Engineering, University of Massachusetts, 2001.
(12) Elkovitch, M. D.; Tomasko, D. L.; Lee, L. J. *Polym. Eng. Sci.* **1999**, *39*, 2075−2084.
(13) Shi, C.; DeSimone, J. M.; Kiserow, D. J.; Roberts, G. W. *Macromolecules* **2001**, *34*, 7744−7750.
(14) Antonietti, M.; Coutandin, J.; Grutter, R.; Sillescu, H. *Macromolecules* **1984**, *17*, 798−802.
(15) Antonietti, M.; Coutandin, J.; Sillescu, H. *Makromol. Chem., Rapid Commun.* **1984**, *5*, 525−528.
(16) Green, P. F.; Palmstrom, C. J.; Mayer, J. W.; Kramer, E. J. *Macromolecules* **1985**, *18*, 501−507.
(17) Green, P. F.; Kramer, E. J. *J. Mater. Res.* **1986**, 202−204.
(18) Amis, E. J.; Han, C. C.; Matsushita, Y. *Polymer* **1984**, *25*, 650−658.
(19) Callaghan, P. T.; Pinder, D. N. *Macromolecules* **1981**, *14*, 1334−1340.
(20) Cosgrove, T.; Warren, R. F. *Polymer* **1977**, *18*, 255−258.
(21) Leger, L.; Hervet, H.; Rondelez, F. *Macromolecules* **1981**, *14*, 1732−1738.
(22) Wesson, J. A.; Noh, I.; Kitano, T.; Yu, H. *Macromolecules* **1984**, *17*, 782−792.
(23) Nemoto, N.; Kojima, T.; Inoue, T.; Kishine, M.; Hirayama, T.; Kurata, M. *Macromolecules* **1989**, *22*, 3793−3798.
(24) Nemoto, N.; Kishine, M.; Inoue, T.; Osaki, K. *Macromolecules* **1991**, *24*, 1648−1654.
(25) Gennes, P. G. D. *J. Chem. Phys.* **1971**, *55*, 572−579.
(26) Doi, M.; Edwards, S. F. *The Theory of Polymer Dynamics*, 1st ed.; Oxford Science Publications: Oxford, 1986.
(27) Lodge, T. P.; Rotstein, N. A.; Prager, S. *Adv. Chem. Phys.* **1990**, *79*, 1−132.
(28) Kausch, H. H.; Tirrell, M. *Annu. Rev. Mater. Sci.* **1989**, *19*, 341−377.
(29) Tirrell, M. *Rubber Chem. Technol.* **1984**, *57*, 523−556.
(30) Klein, J. *Nature (London)* **1978**, *271*, 143−145.
(31) Richter, D.; Farago, B.; Fetters, L. J.; Huang, J. S.; Ewen, B.; Lartigue, C. *Phys. Rev. Lett.* **1990**, *64*, 1389−1392.
(32) Russell, T. P.; Deline, V. R.; Dozier, W. D.; Felcher, G. P.; Agrawal, G.; Wool, R. P.; Mays, J. W. *Nature (London)* **1993**, *365*, 235−237.
(33) Green, P. F. Ion Beam Analysis of Diffusion in Polymer Melts. Ph.D. in Material Science, Cornell University, 1985.
(34) Berry, G. C.; Fox, T. G. *Adv. Polym. Sci.* **1968**, *5*, 261−357.
(35) Gennes, P. G. D. *Macromolecules* **1976**, *9*, 587−593.
(36) Gennes, P. G. D. *Macromolecules* **1976**, *9*, 594−598.
(37) Lodge, T. P. *Phys. Rev. Lett.* **1999**, *83*, 3218−3221.
(38) Tao, H.; Lodge, T. P.; von Meerwall, E. D. *Macromolecules* **2000**, *33*, 1747−1758.
(39) Russell, T. P. X-ray and Neutron Reflectivity for the Investigation of Polymers, Material Science Report, 1990.
(40) Bucknall, D. G.; Butler, S. A.; Higgins, J. S. *Macromolecules* **1999**, *32*, 5453−5456.
(41) Karim, A.; Felcher, G. P.; Russell, T. P. *Macromolecules* **1994**, *27*, 6973−6979.
(42) Schnell, R.; Stamm, M.; Creton, C. *Macromolecules* **1998**, *31*, 2284−2292.
(43) Karim, A.; Mansour, A.; Felcher, G. P.; Russell, T. P. *Phys. Rev. B* **1990**, *42*, 6846−6849.
(44) Ferry, J. D. *Viscoelastic Properties of Polymers*, 2nd ed.; John Wiley & Sons Inc.: New York, 1970.
(45) Osaki, K.; Nishimura, Y.; Kurata, M. *Macromolecules* **1985**, *18*, 1153−1157.
(46) RamachandraRao, V. S.; Gupta, R. R.; Russell, T. P.; Watkins, J. J. Manuscript in preparation.
(47) Cohen, M. H.; Turnbull, D. *J. Chem. Phys.* **1959**, *31*, 1164−1169.
(48) Turnbull, D.; Cohen, M. H. *J. Chem. Phys.* **1961**, *34*, 120−125.
(49) Fujita, H. *Fortschr. Hochpolym., Forsch.* **1961**, *3*, 1−47.
(50) Vrentas, J. S.; Duda, J. L. *Macromolecules* **1976**, *9*, 785−790.
(51) Vrentas, J. S.; Duda, J. L. *J. Polym. Sci.* **1977**, *15*, 403−416.
(52) Vrentas, J. S.; Duda, J. L. *J. Polym. Sci., Polym. Phys.* **1977**, *15*, 417−439.
(53) Alsoy, S.; Duda, J. L. *AIChE J.* **1998**, *44*, 582−590.
(54) Gupta, R. R.; RamachandraRao, V. S.; Watkins, J. J. Manuscript in preparation.
(55) Wissinger, R. G.; Paulaitis, M. E. *J. Polym. Sci., Polym. Phys. Ed.* **1987**, *25*.
(56) Chapman, B. R.; Gochanour, C. R.; Paulaitis, M. E. *Macromolecules* **1996**, *29*, 5635−5649.
(57) Chow, T. S. *Macromolecules* **1980**, *13*, 362−364.
(58) Chapman, B. R. Probe Diffusion in $CO_2$-Plasticized Glassy Polystyrene across the Glass Transition by Forced Rayleigh Scattering. Ph.D. in Chemical Engineering, University of Delaware, 1997.
(59) Wissinger, R. G.; Paulaitis, M. E. *J. Polym. Sci., Part B: Polym. Phys.* **1991**, *29*, 631−633.
(60) Reiter, G.; Steiner, U. *J. Phys. 2* **1991**, 659−671.
(61) Whitlow, S. J.; Wool, R. P. *Macromolecules* **1989**, *22*, 2648−2652.
(62) Ganesh, K.; Nagarajan, R.; Duda, J. L. *Ind. Eng. Chem. Res.* **1992**, *31*, 746−755.


MA021215R